Article

Not peer-reviewed version

Insights into the Replication Kinetics Profiles of Malaysian SARS-CoV-2 Variant Alpha, Beta, Delta, and Omicron in Vero E6 cell line

Zarina Mohd Zawawi *, Jeevanathan Kalyanasundram, Rozainanee Mohd Zain, Adiratna Mat Ripen, Dayang Fredalina Basri, Wei Boon Yap *

Posted Date: 13 August 2024

doi: 10.20944/preprints202408.0950.v1

Keywords: SARS-CoV-2; variants; replication kinetics; infectivity; mutations; cell culture adaptation

 doi:10.20944/preprints202408.0950.v1

Article

Insights into the Replication Kinetics Profiles of Malaysian SARS-CoV-2 Variant Alpha, Beta, Delta, and Omicron in Vero E6 Cell Line

Zarina Mohd Zawawi [1,2,*], Jeevanathan Kalyanasundram [1], Rozainanee Mohd Zain [1], Adiratna Mat Ripen [3], Dayang Fredalina Basri [4] and Wei Boon Yap [2,5,*]

[1] Virology Unit, Infectious Disease Research Centre, Institute for Medical Research, National Institutes of Health, Ministry of Health, 40170 Shah Alam, Selangor, Malaysia.
[2] Center for Toxicology and Health Risk Studies, Faculty of Health Sciences, Universiti Kebangsaan Malaysia, 50300 Kuala Lumpur, Malaysia.
[3] Cancer Research Centre, Institute for Medical Research, National Institutes of Health, Ministry of Health, 40170 Shah Alam, Selangor, Malaysia.
[4] Center for Diagnostic, Therapeutic and Investigative Studies, Faculty of Health Sciences, Universiti Kebangsaan Malaysia, 50300 Kuala Lumpur, Malaysia.
[5] One Health UKM, Universiti Kebangsaan Malaysia, 43600 UKM Bangi, Selangor, Malaysia.
* Correspondence: zarina.zawawi@moh.gov.my (Z.M.Z.); yapweiboon@ukm.edu.my (W.B.Y.)

Abstract: Comprehending the replication kinetics of SARS-CoV-2 variants helps explain why certain variants spread more easily and are more contagious, and pose significant health menaces to the global populations. The replication kinetics of Malaysian isolates of the Alpha, Beta, Delta, and Omicron variants were studied in the Vero E6 cell line. Their replication kinetics were determined using the plaque assay, quantitative real-time PCR (qRT-PCR), and viral growth curve. The Beta variant exhibited the highest replication rate at 24 hours post-infection (h.p.i), as evidenced by the highest viral titers and lowest viral RNA multiplication threshold. The plaque phenotypes also varied among the variants, in which the Beta and Omicron variants formed the largest and smallest plaques, respectively. All studied variants showed strong cytopathic effects after 48 h.p.i. The whole-genome sequencing highlighted cell-culture adaptation, where the Beta, Delta and Omicron variants acquired mutations at the multibasic cleavage site after three cycles of passaging. The findings suggest a strong link between the replication rates and their respective transmissibility and pathogenicity. This is essential in predicting the impacts of the upcoming variants on the local and global populations and is useful in designing preventive measures to curb the virus outbreaks.

Keywords: SARS-CoV-2; variants; replication kinetics; infectivity; mutations; cell culture adaptation

1. Introduction

Severe acute respiratory syndrome coronavirus 2 (SARS-CoV-2) is the causative agent responsible for the COVID-19 pandemic causing millions of deaths and morbidity globally including Malaysia. It belongs to the *Betacoronavirus* family and is closely related to SARS-CoV virus that was first documented in November 2002-2003 [1]. Malaysia reported the emergence of Alpha and Beta variants during the third wave of the pandemic, whereas the Delta (B.1.617.2) variant dominated the fourth wave but later was replaced by AY.59 and AY.79 in Peninsular Malaysia and AY.23 in East Malaysia. The Omicron variant (BA.1 lineage) emerged in December 2021 during the fifth wave [2,3]. The mutational rate of SARS-CoV-2 was estimated to be around 1×10^{-6} to 2×10^{-6} mutations per site per generation [4]. This rapid mutation is attributed to factors such as lack of proofreading by the viral RNA-dependent RNA polymerase (RdRp) and selective pressures from the host immune response. The situation was worsened by the extensive global spread that created abundant opportunities for the accumulation of virus particles in infected

 doi:10.20944/preprints202408.0950.v1

individuals, which in turn resulted in successful evolution of SARS-CoV-2 [5]. This genetic diversity subsequently leads to the emergence of variants with distinctive phenotypic characteristics, increased transmissibility, disease severity, and immune evasion.

Throughout the pandemic, the wild-type SARS-CoV-2 virus has evolved to form numerous pathogenic and contagious variants. Despite the complexity of the viral evolution, certain general insights have been deduced. The Alpha variant (B.1.1.7), identified in the United Kingdom in September 2020, is primarily characterized by the N501Y mutation along with the common D614G mutation in the S protein hence increased transmissibility [6]. In December 2020, the Beta variant (B.1.351) emerged in South Africa with a number of significant mutations (N501Y, E484K, and K417N) that affected the binding of neutralizing antibodies, therefore conferring resistance to monoclonal antibodies [7,8]. The Delta variant (B.1.617.2), on the other hand, emerged in India in late 2020 or early 2021 and was shown to be 40–60% more transmissible. The Delta variant carried a few mutations (L452R, P681R, and T478K) that impacted on the host immunity, viral entry, infectivity, and transmissibility [9]. The Omicron variant (B.1.1.529) emerged in South Africa in November 2021 and possessed over 60 mutations. More than half of the mutations were found in the S protein, including key mutations in the receptor-binding domain (RBD) such as Δ69–70 deletion, T95I, G142D/Δ143–145 deletion, K417N, T478K, N501Y, N655Y, N679K, and P681H [10]. The mutations modified the structure of the S protein and its RBD, and deteriorated the neutralizing antibody binding. As a result, the virus transmissibility and infectivity, and ability to evade host immunity were heightened in relative to the Delta variant of SARS-CoV-2.

The impact of viral genome mutations on viral transmissibility and infectivity can be reflected in the virus replication profile [11]. An efficient virus replication promotes viral loads in bodily fluids, which in turn facilitates the virus shedding and transmission. Moreover, the higher viral load also can induce extensive tissue damage and a stronger immune response, and leads to increased pathogenicity [12]. Therefore, dissecting the replication kinetics of various Malaysian SARS-CoV-2 variants is crucial for assessing the impacts of the virus infections on patients, as well as serving as a guide for improving the control and preventive measures of the virus outbreaks. To better understand the relationship between the replication kinetics of SARS-CoV-2 Alpha, Beta, Delta, and Omicron variants and their pathogenicity, the virus infections were performed in African Green Monkey-derived Vero E6 kidney cell line in this study. The Vero E6 cell line has been widely used in coronavirus research as it is highly susceptible to coronavirus infections such as SARS-CoV and SARS-CoV-2 and therefore supports coronavirus replications and enables high viral load synthesis [13,14]. Although lacking the TMPRSS2 protease required for virus entry, Vero E6 cells express angiotensin-converting enzyme 2 (ACE2) receptor for SARS-CoV-2 attachment [15]. In addition, their deficiency in interferon production allows robust viral replication without host antiviral interference [16]. Altogether, Vero E6 cell line is an eligible host cell model for studying and comparing the replication dynamics of SARS-CoV-2 variants.

Rosli et al (2023) investigated the growth profiles of Malaysian SARS-CoV-2 strains (clades L/Lineage B Wuhan, GR/Lineage B.1.1.354, and O/Lineage B.6.2) collected in the early of COVID-19 pandemic in various mammalian cell lines, including Vero E6, Vero CCL-81 and Calu-3 [17]. Although the growth profiles of the variants were reportedly cell line-dependent, the study lacked a clear and direct comparison between the studied variants. Given the replication kinetic and virus infectivity are highly associated with the unique mutations in the spike proteins of the individual variants, this study aimed to investigate and compare the replication profiles of Malaysian strains of SARS-CoV-2 Alpha, Beta, Delta, and Omicron variants in Vero E6 cell line.

2. Results

2.1. Morphology Changes of Vero E6 Cells Infected with Malaysian SARS-CoV-2 Variants

All four SARS-CoV-2 variants (Alpha, Beta, Delta, and Omicron) formed cytopathic effect (CPE) through cell lysis in Vero E6 cells. The CPE started to appear at 24 h.p.i. and became more severe after 48 h.p.i. [Figure 1(a)]. At 48 h.p.i., approximately 70-80% of the cells were rounded, detached, and lysed. By 72 h.p.i., all infected cells were lysed and floating on the surface of the media.

 doi:10.20944/preprints202408.0950.v1

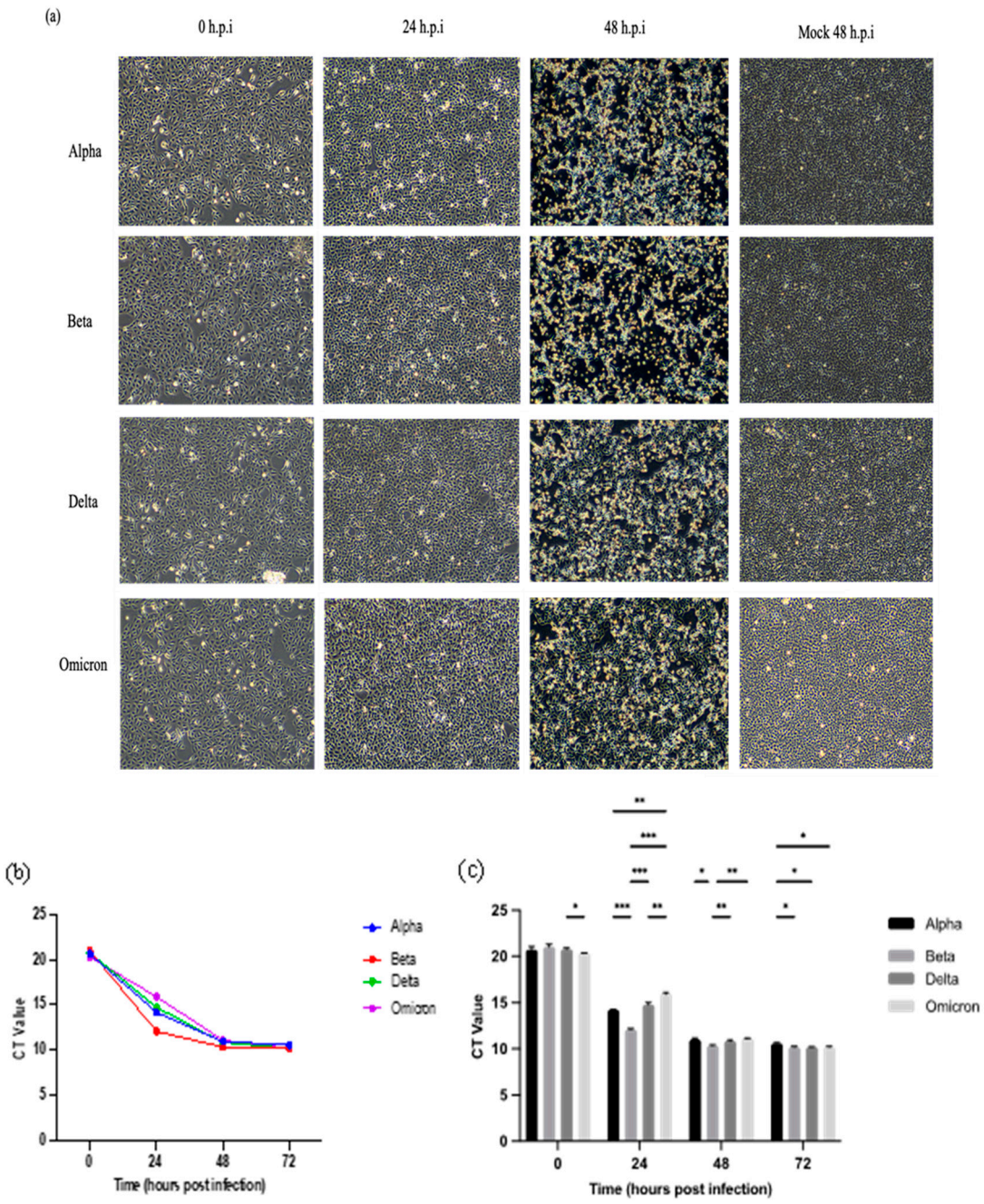

Figure 1. Cytopathic effects (CPE) in Vero E6 cells inoculated with SARS-CoV-2 variants at MOI of 0.001 and detection of SARS-CoV-2 ORF1ab gene in the culture supernatants at the designated time points using qRT-PCR. (a) Representative images of infected Vero E6 cells. CPE were remarkably evident at 48 h.p.i. for all variants. The morphology changes of infected cells were visualized at 100x magnification. (b) RNA genome multiplication trend of the variants. (c) Comparison of Ct values at the designated time points. All four variants exhibited almost similar trends in RNA multiplication. At 24 h.p.i, the Beta variant showed the lowest Ct value followed by the Alpha and Delta variants, the Omicron variant demonstrated the highest Ct value among the variants. The Ct values became plateau after 48 h.p.i. The data values represent the mean ± SD derived from 3 independent experiments. The statistical analysis was performed with the Two-way ANOVA and Tukey's multiple comparison tests. *$p < 0.033$, **$p < 0.002$, and ***$p < 0.001$.

 doi:10.20944/preprints202408.0950.v1

2.2. Viral RNA Multiplication of SARS-CoV-2 Variants in Vero E6 Cells

Vero E6 cells were infected with the SARS-CoV-2 variants at MOI 0.001. The Ct values of the variants harvested at designated post-infection time points were determined using qRT-PCR up to 72 h.p.i. Figure 1(b,c) show that the viral loads of the variants increased in the time-dependent manner. Among the four SARS-CoV-2 variants, the Beta variant exhibited significantly higher replication efficiency than the other variants as indicated by the lowest Ct values especially that of 24 h.p.i. Meanwhile, the Omicron variant recorded the highest Ct value at 24 h.p.i. The Ct values of all variants started to become plateau from 48 to 72 h.p.i.

2.3. Plaque Formation and Phenotypes

Figure 2 illustrates the plaque phenotypes and replication kinetics of the four SARS-CoV-2 variants. In the plaque assay [Figure 2(a)], it was shown that the Beta variant formed the largest plaques, followed by the Alpha and Delta variants. The Omicron variant produced the smallest plaques as seen in the well. Visible plaques were observed on day-3 (72 hours) p.i with the Alpha, Beta, and Delta variants; nonetheless, the plaque formation was delayed for 24 hours with the Omicron variant. Unlike the other variants whose plaque phenotypes were relatively consistent, the Alpha variant demonstrated a rather mixed plaque phenotype with both large and small plaques.

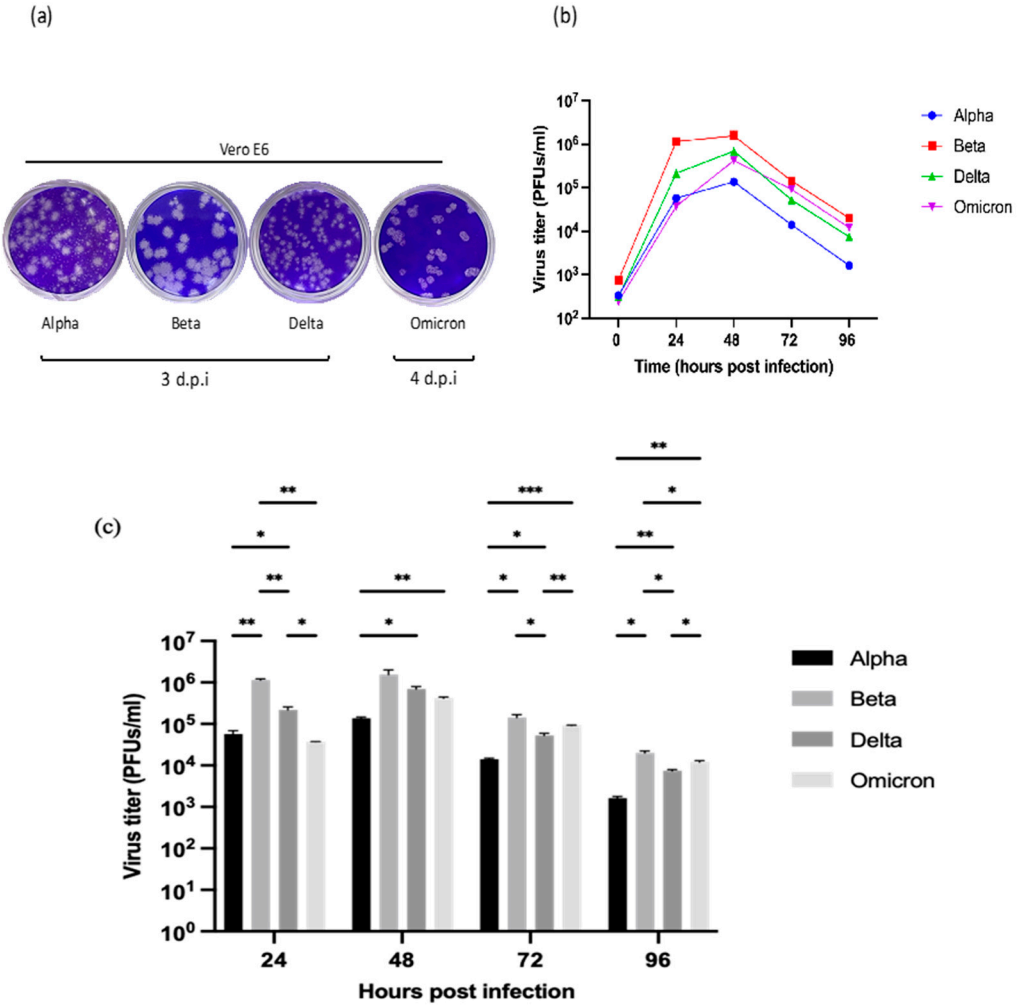

Figure 2. The morphology of plaques and titration of the Alpha, Beta, Delta, and Omicron variants in the Vero E6 cell line. (a) Representative images of the plaque assay. The Beta variant formed larger clear zones than the Alpha, Delta, and Omicron variants. The formation of visible plaques by the Omicron variant was delayed. (b) The titers of the SARS-CoV-2 variants (PFUs/ml). The supernatant was harvested at the designated time points and the virus titers of the samples were determined using the plaque assay. The titers of all four variants peaked at 48 h.p.i with the Beta variant showing the

 doi:10.20944/preprints202408.0950.v1

highest titer. (c) Comparison of the virus titers among the four variants. At 24 h.p.i, the Beta variant produced a significantly higher level of infectious virions than the others. The data values represent the mean ± SD derived from three independent experiments. The statistical analysis was performed with the Two-way ANOVA and Tukey's multiple comparison tests. *$p < 0.033$, **$p < 0.02$, and ***$p < 0.001$.

2.4. Replication Kinetics of SARS-CoV-2 Variants in Vero E6 Cells

Subsequently, the viral titers of all SARS-CoV-2 variants were determined in Vero E6 cells. By comparing the viral titers at the designated time points [Figure 2(b)], the replication patterns of the variants were almost similar. At 24 h.p.i, the replication of all variants increased drastically. The Beta variant already exhibited a significantly higher virus titer ($p < 0.002$) than the other variants at 24 h.p.i [Figure 2(c)]. The viral titers peaked at 48 h.p.i., indicating the maximum viral replication rates. Following the peak, declined viral titers were observed, continuing through to 96 h.p.i. This trend suggests a dynamic interaction between the viral replication and host cellular responses, leading to the reduction of viral loads. Collectively, the results imply that the distinctive replication patterns are variant-specific, and the virus replication dynamics could change over time.

2.5. Whole-Genome Sequencing of SARS-CoV-2 Alpha, Beta, Delta, and Omicron Variants

Given that mutations in the S protein of SARS-CoV-2 can severely impact on the virus transmissibility and pathogenicity, the Next-Generation sequencing (NGS) was conducted using the Oxford Nanopore GridION system to determine the genome stability of the variants after three cycles of passaging. The whole-genome sequences of the variants were aligned and compared with their original sequences [Table 1] using Nextclade v3.8.2.

The results revealed that the Beta, Delta, and Omicron variants exhibited cell culture adaptations in which deletion mutations were detected at the S1/S2 boundary [Figure 3(a,b)]. Several point mutations either by deletion or substitution were found in the multibasic cleavage sites (MBCS) of the S proteins: (i) Beta - N679del, S680del, P681del, R683del, A684del, and R685del; (ii) Delta - Q677del, T678del, N679del, and S680del; and (iii) Omicron - R682W [Figure 3(b)]. The Alpha variant appeared to be relatively stable as there were no additional mutations identified in the variant's MBCS after three cycles of passaging.

Table 1. A list of unique mutations, either by amino acid (aa) substitution or deletion, found in the S protein of each variant after three cycles of passaging (P3) in comparison to their original sequences. The Beta and Delta variants showed additional aa deletion mutations (in bold), whereas the Omicron variant demonstrated an aa substitution (in bold). The Alpha variant maintained its genome stability throughout the passaging in the Vero E6 cell line.

Mutations	Alpha (original)	Alpha (P3)	Beta (Original)	Beta (P3)	Delta (Original)	Delta (P3)	Omicron (Original)	Omicron (P3)
aa substitution	N501Y,A570D, D614G,P681H, T716I,S982A, D1118H	N501Y,A570D, D614G,P681H, T716I,S982A, D1118H	A27S,D80A,D215G, K417N,E484K, N501Y,D614G, A701V	A27S,D80A,D215G, K417N,E484K, N501Y,D614G, A701V	T19R,G142D,R158G, A222V,L452R, T478K,D614G,P681R, D950N	T19R,G142D,R158G, A222V,L452R, T478K,D614G,P681R, D950N	A67V,T95I,Y145D, L212I,G339D, R346K,S371L,S373P, S375F,K417N, N440K,G446S,S477N, T478K,E484A,Q493R, G496S,Q498R,N501Y, Y505H,T547K,D614G, H655Y,N679K,P681H, N764K,D796Y,N856K, Q954H,N969K,L981F	A67V,T95I,Y145D, L212I,G339D, R346K,S371L,S373P, S375F,K417N, N440K,G446S,S477N, T478K,E484A,Q493R, G496S,Q498R,N501Y, Y505H,T547K,D614G, H655Y,N679K,P681H, **R682W**,N764K, D796Y,N856K,Q954H, N969K,L981F
aa deletion	H69-,V70-,Y144-	H69-,V70-, Y144-	L241-,L242-,A243-	L241-,L242-,A243-, **N679-,S680-, P681-, R683-,A684-, R685-**	E156-,F157-	E156-,F157-,**Q677-, T678-, N679-, S680-**	H69-,V70-,G142-, V143-,Y144-,N211-	H69-,V70-,G142-, V143-,Y144-,N211-

doi:10.20944/preprints202408.0950.v1

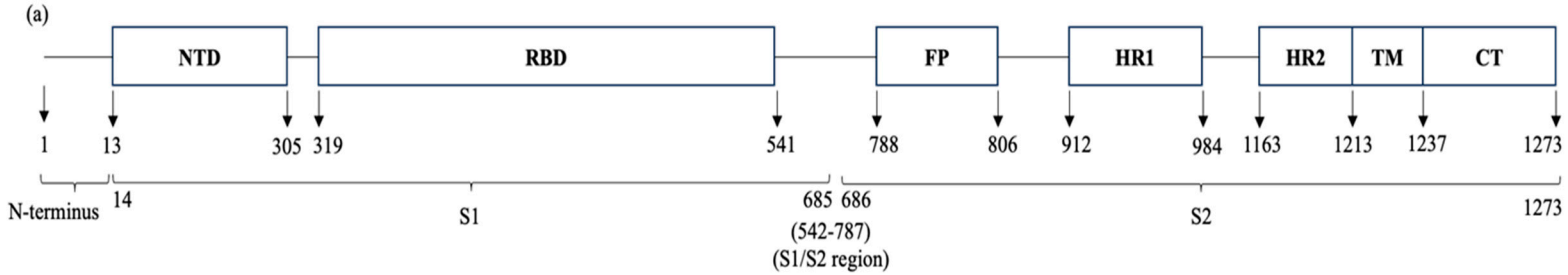

(b)

Codon	675	676	677	678	679	680	681	682	683	684	685	686	687
MN908947.3 (Wuhan-Hu-1) Ref. aa	Q	T	Q	T	N	S	P	R	R	A	R	S	V
Alpha variant (original)	Q	T	Q	T	N	S	H	R	R	A	R	S	V
Alpha variant (P3)	Q	T	Q	T	N	S	H	R	R	A	R	S	V
Beta variant (Original)	Q	T	Q	T	N	S	P	R	R	A	R	S	V
Beta variant (P3)	Q	T	Q	T	*	*	*	R	*	*	*	S	V
Delta variant (Original)	Q	T	Q	T	N	S	R	R	R	A	R	S	V
Delta variant (P3)	Q	T	*	*	*	*	R	R	R	A	R	S	V
Omicron variant (Original)	Q	T	Q	T	K	S	H	R	R	A	R	S	V
Omicron variant (P3)	Q	T	Q	T	K	S	H	W	R	A	R	S	V

Figure 3. A schematic view of the SARS-CoV-2 spike (S) gene and the locations of mutations after cell culture adaptations. (a) The S protein consists of 1273 amino acid (aa); 1 – 13 aa (a single peptide located at the N-terminus), 14 – 685 aa (S1 subunit) and 686 – 1273 aa (S2 subunit). Generally, the S1 and S2 domains are responsible for receptor binding and membrane fusion of SARS-CoV-2 virus into the host cell, respectively. The whole-genome sequencing revealed that the Beta, Delta and Omicron variants possessed mutations in the S1/S2 region when compared to their original sequences [Alpha (B.1.1.7, EPI-ISL-877228), Beta (B.1.351, EPI-ISL-4730383), Delta (AY.59, EPI-ISL-3425462) and Omicron (BA.1.1, EPI-ISL-11105858)]. (b) The Beta and Delta variants were found to carry deletion mutations at the multibasic cleavage site [^{677}QTNSPRRAR^{685}]. The amino acid substitution was reported in the Omicron (R682W) variant. NTD: N terminal domain, RBD: Receptor binding domain, FP: Fusion peptide, HR1: heptapeptide repeat sequence 1, HR2: heptapeptide repeat sequence 2, TM: TM domain, CT: Cytoplasm domain. * aa deletion.

doi:10.20944/preprints202408.0950.v1

 doi:10.20944/preprints202408.0950.v1

3. Discussion

Similar to the other global variants, Malaysian isolates of SARS-CoV-2 variants possibly exhibit differences in their replication kinetics [18]. It is generally accepted that variants with higher abilities in synthesizing infective virions are associated with greater transmissibility and infectivity [19]. In this study, four variants namely Alpha, Beta, Delta, and Omicron sampled in Malaysia during the COVID-19 pandemic were studied and compared. Notably, in Vero E6 cells, all SARS-CoV-2 variants exhibited strong cytopathic effects (CPE) after 48 h.p.i. in the form of cell lysis. The severity of CPE became more visible over the incubation period, particularly at 48 h.p.i. due to extensive virus-induced cell damages; it limited the replication of the variants as implied by the constant Ct values and declined viral titers at 48-72 and 48-96 h.p.i., respectively. In this study, the viral titers were monitored up to 96 h.p.i. to better decipher the replication patterns of the variant, which increased at 24 h.p.i. and culminated at around 48 h.p.i. and subsequently declined at 72-96 h.p.i., thereby providing insights into the duration of infectivity. Whereas, monitoring the viral RNA multiplication thresholds beyond 72 h.p.i. did not provide additional information on the replication dynamics of the variants as their RNA levels were already plateau by that point.

The plaque size can serve as an indication of the transmissibility or contagiousness of the variants. The variants exhibited plausible variations in the plaque size, which was correlated with the RNA multiplication threshold and virus titer of the variants. In this study, the Beta variant formed the largest plaques, yielded the highest number of RNA multiplication (lowest Ct value) and virus titers at 24 and 48 h.p.i. This suggests that the Beta variant demonstrated a higher viral replication rate and infectivity [20]. Similar findings were also reported by several previous studies [21–23] comparing the replication kinetics of the Beta variant to that of the Alpha and a few other variants. The Beta variant was also reported to form larger plaques and demonstrate higher thermal stability, hence an increased viral replication rate. The greater replication and infectivity of the Beta variant was linked to its E484K mutation in the S protein, which caused reduced antibody neutralization, and A701V mutation that impaired the attachment of the S protein to the ACE2 receptor [24]. As a result, those unique mutations (E484K and A701V) were likely to provide a fitness advantage to the Beta variant, making it globally dominant before the emergence of the later variants.

In contrast, the Alpha variant was shown to form smaller plaques with mixed phenotypes and exhibited relatively lower viral replication and infectivity than the other variants. The differences were remarkably evident compared to that of the Beta variant. This is in line with that reported by Jeong et al. [23] in which the Alpha variant also produced smaller plaques, fewer infectious viral particles and resulted in a lower intracellular viral RNA concentration than the Beta, Gamma, and Delta variants. However, in comparison with the wild-type (wt) SARS-CoV-2, the Alpha variant demonstrated an improved replication kinetic due to the presence of D614G and N501Y mutations [25] and impairment of type-1 interferon activities by the P681H mutation in the S protein [26].

Similarly, the Delta variant also exhibited smaller plaque formation. This is consistent with the findings reported by Tanneti et al. [27], which showed that both the Alpha and Delta variants produced significantly smaller plaques in Vero E6 TMPRSS2 cells. Regardless the smaller plaque formation, the Delta variant still could yield significantly higher infectious viral titers at 24 and 48 h.p.i in this study. This finding contradicts that of Tandel et al. [28], who reported that the Delta variant demonstrated a higher RNA replicative fitness but produced a lower infectious viral titer. Mautner et al. [18] also reported differing results in their comparative analysis on the replication kinetics and infectivity of the Alpha, Beta, Delta, and Omicron variants in the Vero E6 and CaCo2 cell models. They found that in Vero E6 cells, the titer of the Alpha variant (TCID50/mL) was higher than the Delta variant after 24 h.p.i., which is consistent with the findings of this study. However, in CaCo2 cells, the Alpha variant formed a lower titer than the Delta variant. This discrepancy may be due to differences in the host cell tropisms as the CaCo2 is a colon adenocarcinoma cell line whereas the Vero E6 is an African green monkey non-carcinoma kidney cell line.

Despite being the currently circulating variant globally, the Omicron variant demonstrated slower replicative ability than the other studied variants in this study. The formation of visible plaques was also delayed (about 4 to 5 days) compared to its fraternity variants. Shuai et al. [29] discovered that the Omicron variant replicated less efficiently than the wt SARS-CoV-2, Alpha, Beta,

 doi:10.20944/preprints202408.0950.v1

and Delta and caused comparatively lower cellular damages. The slower replication kinetics of the Omicron variant can be attributed to several factors, among others, the altered entry pathway that favours endocytosis over the plasma membrane route [30]. In addition, the Omicron variant is also less effective in inhibiting the host cell's innate immune response than the Delta variant. This explains its slower replication due to its relatively higher sensitivity to the antiviral immunity of host cells [31]. Collectively, the Omicron variant exhibits low fusogenic potential, which reduces cell-to-cell spread and impacts on the efficiency of viral replication and virus spread [32]. This also explains why it took longer for the Omicron variant to form visible plaques than the Alpha, Beta and Delta variants.

Reduced fusogenicity is associated with milder disease progression as seen in Omicron-infected patients [33]. This phenomenon is linked to its unique H655Y [34] and N856K [35] mutations in the S protein. The H655Y mutation stabilizes the spike trimer conformation that is important for viral entry into host cells [34]. This in turn decreases the flexibility of the S protein through hydrophobic interactions with specific residues. The loss of plasticity of the S protein interferes with the furin cleavage site and affects envelope-membrane fusion. According to Sun et al. [35], when the N856K substitution was introduced in the spike of Omicron BA.1, it was 9.2- and 11.9-fold less fusogenic than the Delta or D614G variant, respectively. The aforementioned H655Y and N856K mutations were also observed in the Omicron variant of this study [Table 1]. The substitutions are believed to potentially prevent the release of the spike protein and obstruct the conformational change of the spike, and it, therefore, explains the delayed plaque formation and lower viral titer due to the lower fusogenicity of the Omicron variant observed at 24 h.p.i.

Park et al. [36] investigated and compared the fusogenicity of the Omicron BA.1 variant with the other earlier lineages (Alpha, Beta, Delta) and noted that the fusogenic activities were proportional to the infectivity of the variants. The study attributed the reduced fusogenicity and infectivity of Omicron BA.1 to the unique mutations in the S1 and S2 domains [36]. Similarly, in this study, Figure 3(b) shows that the Omicron variant exhibited substitution mutations of N679K and P681H in the S1/S2 domain, which were not present in the Alpha, Beta and Delta variants. In addition, Park et al. [36] also identified and reported five additional mutations (T547K, H655Y, N856K, Q954H, N969K) in the viral S protein that were responsible for the reduced fusogenicity of Omicron BA.1. This finding is consistent with that listed in Table 1. It is, therefore, noteworthy that the presence of multiple mutations in the S protein of the Omicron variant especially in the S1/S2 region may reduce membrane fusion between the virions and host cells, and subsequently lower the impact of the virus infection.

In this study, the whole-genome sequencing was performed to investigate the genome stability and cell culture adaptability of the variants after three cycles of passaging. Their sequences were aligned and compared with that of the original clinical samples. The results revealed several amino acid deletion mutations at the multibasic cleavage sites (MBCS) in the S proteins of the Beta and Delta variants, specifically at the furin cleavage site (^{677}QTNSPRRAR^{685}). The Omicron variant acquired only an amino acid substitution of R682W at the MBCS. Mutations at the MBCS can affect the entry mode of the variants, i.e. the endosomal pathway (slower) or the cell-surface pathway (faster) as the entry mode of choice is largely dependent on the proteolytic activities of the TMPRSS2 protein at the MBCS [37]. As a result, any mutations altering the proteolytic reactions of TMRPSS2 at the MBCS can eventually modify the fusogenicity of infectious virions with the host cell membrane. In addition, the frequency of TMPRSS2 present on the host cell surface also affects the mode of viral entry. When the number of TMPRSS2 is low or negligible, the virus executes the slower endosomal entry pathway and vice versa. Therefore, to accommodate the absence of TMPRSS2 protease on Vero E6 cells, SARS-CoV-2 variants swiftly adapt themselves through genome mutations, particularly at the furin cleavage site so that they can perform alternative endosomal entry. This adaptation enhances the viral fitness or replication in the absence of the TMPRSS2-mediated pathway [38].

Introducing novel amino acid motifs, such as PRRA and QTQTN of SARS-CoV-2 S protein into that of SARS-CoV drastically affects the virus entry into host cells and impacts the infectivity and transmissibility of SARS-CoV [39]. This implies the importance of PRRA and QTQTN motifs in concerting the entry of SARS-CoV-2 variants as demonstrated in this study. Romeu (2023) also suggested that the acquired PRRA furin polybasic motif was a key evolutionary step leading to the

 doi:10.20944/preprints202408.0950.v1

emergence of the pandemic coronavirus. The PRRA of SARS-CoV-2 showed almost 100% similarity with that of the human RNA [40]. This scenario indicates a potential recombination event between the virus genome and human RNA.

In this study, the Beta and Delta variants exhibited amino acid deletions specifically at ^{679}NSP-RAR^{685} and ^{677}QTNS^{680}, respectively after three consecutive passaging. Liu et al. [41] reported that residue deletions usually occurred after two cycles of passaging. The study found the QTQTN deletion in clinical samples and laboratory-adapted virus isolates, and the NSPRRAR deletion in the laboratory-adapted isolates using the Oxford Nanopore Technologies (ONT) platform. However, their empirical findings indicated that the NSPRRAR deletion was less likely to impact the virus replication in Vero and Vero-E6 cells; the QTQTN deletion, on the other hand, may restrict the late-phase viral replication [41]. The findings were somehow contradictory to that of Davidson et al. [42] in which mutations that altered or deleted the putative furin cleavage site could lead to a significant change in the virus replication. Considering those previous findings, it is speculated that deletions at those specific sites may have varying effects on the viral replication, both in cell culture and clinical samples. In this study, the effects of ^{679}NSP-RAR^{685} deletion in the Beta variant were similar to that reported previously [21–23]. The mutation did not significantly affect the viral replication and infectivity as indicated by the plaque size and replication of the Beta variant. However, the smaller plaque formed by the Delta variant may be attributed to the ^{677}QTNS^{680} deletion and it is consistent with that reported by Tanneti et al. [27]. The deletion likely disturbed the viral replication in the later stages as evidenced by smaller plaque formation, which reflected reduced viral growth and spread within the cell culture. To substantiate how the manipulation of amino acids in the S protein by SARS-CoV-2 variants affects the virus adsorption, entry, and replication as a whole, further bioinformatic and empirical analyses are required.

4. Materials and Methods

4.1. Cell Culture

African green monkey (Vero E6; ATCC CRL-1586) cell line was used in this study. The cells were maintained in Dulbecco's minimal essential medium (DMEM; Nacalai Tesque, Kyoto, Japan) supplemented with 1% penicillin-streptomycin (10,000 U/mL) (Nacalai Tesque, Kyoto, Japan), 25 mM HEPES, L-glutamine and 10% heat-inactivated fetal bovine serum (FBS; Nacalai Tesque, Kyoto, Japan). The cells were passaged every 3 to 4 days by dissociating them with TrypLETM Express Enzyme (Gibco, Grand Island, NE, USA). The cells were incubated at 37°C in 5% CO_2.

4.2. Virus Propagation, Isolation and Preparation of Virus Stocks

SARS-CoV-2 variants including Alpha (B.1.1.7, EPI-ISL-877228), Beta (B.1.351, EPI-ISL-4730383), Delta (AY.59, EPI-ISL-3425462) and Omicron (BA.1.1, EPI-ISL-11105858) were studied. The archived viruses were obtained from the Virology Unit, Institute for Medical Research (IMR), Malaysia Ministry of Health. They were isolated from COVID-19 patients' nasopharyngeal swab samples. All four SARS-CoV-2 variants were confirmed by real-time reverse transcription polymerase chain reaction (qRT-PCR) and Next-Generation sequencing. The virus propagation and isolation were carried out in Vero E6 cells for three passages and stored as virus stocks. The plaque assay was performed to determine the multiplicity of infection (MOI) of the virus stocks and MOI of 0.001 was used in all assays. The above experiments were done in the Biosafety Level 3 facility, IMR.

4.3. Plaque Assay

Titration of viral load in the infectious culture supernatants collected at five different time points was conducted in Vero E6 cells in triplicates. The supernatants were diluted 10 folds from 10^{-1} to 10^{-5} with DMEM without serum. Confluent monolayer Vero E6 cells were prepared a day prior to the plaque assay by seeding 2.5 x 10^5 of Vero E6 cells in 12-well plates and cultured with DMEM supplemented with 10% FBS. On the day of the plaque assay, the growth medium was removed, and the cells were infected with 0.3 mL of 10^{-1} to 10^{-5}-diluted samples. Mock infection was performed using only DMEM without serum and acted as the negative control. The cells were incubated at 37°C, 5% CO_2 for 60 minutes. After

 doi:10.20944/preprints202408.0950.v1

incubation, the virus inoculum was removed, and the cell monolayer were washed and then covered with 1 mL of overlay medium (0.8% w/v agarose: DMEM; 1:3) and allowed to solidify at room temperature. The plates were incubated at 37°C in 5% CO_2 for 3 to 5 days before fixation using 4% paraformaldehyde phosphate buffer solution (Nacalai Tesque, Kyoto, Japan) for 2 hours. The overlay agar was removed under running water and the cell monolayer was stained with 0.5% crystal violet in 25% methanol. Clear plaques were quantified to determine the plaque-forming units per unit volume (PFU/mL).

4.4. Infectivity Assay

Vero E6 cells were seeded in 6-well plates at 5.0 x 10^5 cells/well in DMEM supplemented with 10% FBS a day prior to the infection. The cells were infected with SARS-CoV-2 Alpha, Beta, Delta, and Omicron variants at MOI of 0.001 for 60 minutes, with occasional shaking every 10 to 15 minutes. After adsorption, the media was removed and the cells were washed with phosphate-buffered saline (PBS; Gibco, Paisley, UK). Then, 2 ml of fresh DMEM supplemented with 2% FBS was added to each well. The presence of cytopathic effects (CPE) was observed daily for 5 days. The supernatant was collected at five different time points, i.e. 0, 24, 48, 72 and 96 h.p.i for investigating the virus growth kinetics. Approximately, 200 mL of the supernatants was aliquoted at the designated time points and heat-inactivated for 1 hour. The remaining supernatants served as the infectious culture supernatants. All samples were stored at -80°C until further analyzed in the virus titration assay and viral RNA extraction. All infections were done in triplicates; technically and biologically.

4.5. RNA Extraction and Nucleic Acids Amplification

The total RNA in the culture supernatant was extracted using the QIAamp viral RNA Mini Kit (Qiagen, Hilden, Germany) and the presence of the virus genome was evaluated using qRT-PCR by employing the BGI's Real-Time Fluorescent RT-PCR kit (BGI, Wuhan, China). The amplification was based on the SARS-CoV-2 ORF1ab and N genes.

4.6. Whole Genome Sequencing

The nucleic acid sequences of the variants were sequenced to determine their genomic stability after three passages. The viral RNA was extracted and amplified as described before. Next-generation sequencing (NGS) was performed by using the Oxford Nanopore GridION system (Apical Scientific, Seri Kembangan, Malaysia). Four data sets (Alpha variant, Beta variant, Delta variant, Omicron variant) were obtained and analyzed using the NextClade software (https://clades.nextstrain.org).

4.7. Statistical Analysis

Data values represent the mean ± SD from 3 independent experiments. The statistical analysis was performed using two-way ANOVA and Tukey's multiple comparison test to compare the levels of gene expression and viral titers of four variants at the designated time points. A p-value < 0.05 was considered significant for all statistical tests. All the data were analyzed using the GraphPad Prism 9.0 (GraphPad Software, San Diego, CA, USA.).

5. Conclusions

Overall, the replication kinetics of Alpha, Beta, Delta, and Omicron variants in Vero E6 cells exhibited similar growth patterns. Among the variants, the Beta variant showed the most efficient replication; nonetheless, the Omicron variant displayed a relatively slower replicative ability than its fraternity variants, which is most likely due to its low fusogenic properties. In conclusion, compared to the Omicron variant, the earlier VOCs showed minor variations in their replication kinetics in Vero E6 cells. It, therefore, implies the importance of monitoring the replicative abilities of the circulating and upcoming variants, in addition to their transmissibility, pathogenicity, and immune escape capabilities, in order to promote public health measures in controlling the virus spread. It also is a pivotal measure to monitor genetic variations in the variants, especially in the S1/S2 region of the spike before and after propagating the SARS-CoV-2 variants *in vitro* to ensure genome stability of the working stocks.

 doi:10.20944/preprints202408.0950.v1

Author Contributions: Zarina Mohd Zawawi conceptualized the study, acquired, and analysed the data, prepared, and edited the manuscript draft. Jeevanathan Kalyanasundram, Adiratna Mat Ripen, Dayang Fredalina Basri, Rozainanee Mohd Zain, and Wei Boon Yap conceptualized, reviewed, and finalized the manuscript for submission. Wei Boon Yap, Jee-vanathan Kalyanasundram, Dayang Fredalina Basri supervised the postgraduate student (Zarina Mohd Zawawi) who prepared the manuscript draft. All the authors read and contributed to the completion of the manuscript.

Funding: This work was funded by the Fundamental Research Grant Scheme, Malaysia Ministry of Higher Education (MoHE), (Grant number: FRGS/1/2021/STG03/UKM/02/2), and Ministry of Health, Malaysia (MOH), (Grant number: NMRR ID-22-01257-WCO).

Institutional Review Board Statement: This study was approved by the Ministry of Health Malaysia (MOH) Medical Research and Ethics Committee (reference: 22-01257-WCO).

Informed Consent Statement: Not applicable.

Data Availability Statement: Dataset available on request from the authors.

Acknowledgments: We would like to thank the Director General of Health Malaysia for his permission to publish this article.

Conflicts of Interest: The authors declare no conflict of interest.

References

1. Rahimi, G., Rahimi, B., Panahi, M., Abkhiz, S., Saraygord-Afshari, N., Milani, M., & Alizadeh, E. (2021). An overview of Betacoronaviruses-associated severe respiratory syndromes, focusing on sex-type-specific immune responses. *International Immunopharmacology, 92,* 107365. https://doi.org/10.1016/j.intimp.2021.107365
2. Yu, C. Y., Wong, S. Y., Liew, N. W. C., Joseph, N., Zakaria, Z., Nurulfiza, I., Soe, H. J., Kairon, R., Amin-Nordin, S., & Chee, H. Y. (2022). Whole genome sequencing analysis of SARS-CoV-2 from Malaysia: From alpha to Omicron. *Frontiers in Medicine, 9,* 1001022. https://doi.org/10.3389/fmed.2022.1001022
3. Azami, N. A. M., Perera, D., Thayan, R., AbuBakar, S., Sam, I. C., Salleh, M. Z., Isa, M. N. M., Ab Mutalib, N. S., Aik, W. K., Suppiah, J., Tan, K. K., Chan, Y. F., Teh, L. K., Azzam, G., Rasheed, Z. B. M., Chan, J. C. J., Kamel, K. A., Tan, J. Y., Khalilur Rahman, O., ... Malaysia COVID-19 Genomics Surveillance Consortium. (2022). SARS-CoV-2 genomic surveillance in Malaysia: displacement of B.1.617.2 with AY lineages as the dominant Delta variants and the introduction of Omicron during the fourth epidemic wave. *International Journal of Infectious Diseases, 125,* 216–226. https://doi.org/10.1016/j.ijid.2022.10.044
4. Amicone, M., Borges, V., Alves, M. J., Isidro, J., Zé-Zé, L., Duarte, S., ... & Gordo, I. (2022). Mutation rate of SARS-CoV-2 and emergence of mutators during experimental evolution. *Evolution, Medicine, and Public Health, 10*(1), 142-155.
5. Peacock, T. P., Penrice-Randal, R., Hiscox, J. A., & Barclay, W. S. (2021). SARS-CoV-2 one year on: evidence for ongoing viral adaptation. *Journal of General Virology, 102*(4).
6. Luan, B., Wang, H., & Huynh, T. (2021). Enhanced binding of the N501Y-mutated SARS-CoV-2 spike protein to the human ACE2 receptor: insights from molecular dynamics simulations. *FEBS Letters, 595*(10), 1454-1461.
7. Tegally, H., Wilkinson, E., Giovanetti, M., Iranzadeh, A., Fonseca, V., Giandhari, J., ... & de Oliveira, T. (2021). Detection of a SARS-CoV-2 variant of concern in South Africa. *Nature, 592*(7854), 438-443.
8. Focosi, D., & Maggi, F. (2021). Neutralising antibody escape of SARS-CoV-2 spike protein: risk assessment for antibody-based Covid-19 therapeutics and vaccines. *Reviews in Medical Virology, 31*(6), e2231.
9. Dhawan, M., Sharma, A., Priyanka, Thakur, N., Rajkhowa, T. K., & Choudhary, O. P. (2022). Delta variant (B.1.617.2) of SARS-CoV-2: Mutations, impact, challenges and possible solutions. *Human Vaccines & Immunotherapeutics, 18*(5), 2068883. https://doi.org/10.1080/21645515.2022.2068883
10. Fan, Y., Li, X., Zhang, L., Wan, S., Zhang, L., & Zhou, F. (2022). SARS-CoV-2 Omicron variant: recent progress and future perspectives. *Signal Transduction and Targeted Therapy, 7,* 141. https://doi.org/10.1038/s41392-022-00997-x
11. Hatta, Y., Hershberger, K., Shinya, K., Proll, S. C., Dubielzig, R. R., Hatta, M., ... & Kawaoka, Y. (2010). Viral replication rate regulates clinical outcome and CD8 T cell responses during highly pathogenic H5N1 influenza virus infection in mice. *PLOS Pathogens, 6*(10), e1001139. https://doi.org/10.1371/journal.ppat.1001139

12. Lee, L. Y., Rozmanowski, S., Pang, M., Charlett, A., Anderson, C., Hughes, G. J., ... & Eyre, D. W. (2022). Severe acute respiratory syndrome coronavirus 2 (SARS-CoV-2) infectivity by viral load, S gene variants and demographic factors, and the utility of lateral flow devices to prevent transmission. *Clinical Infectious Diseases, 74*(3), 407-415.
13. Banerjee, A., Nasir, J. A., Budylowski, P., Yip, L., Aftanas, P., Christie, N., ... & Mubareka, S. (2020). Isolation, sequence, infectivity, and replication kinetics of severe acute respiratory syndrome coronavirus 2. *Emerging Infectious Diseases, 26*(9), 2054.
14. Chen, Y., Liu, M. Q., Luo, Y., Jiang, R. D., Si, H. R., Zhu, Y., ... & Yang, X. L. (2021). Genetic mutation of SARS-CoV-2 during consecutive passages in permissive cells. *Virologica Sinica, 36*(5), 1073–1076. https://doi.org/10.1007/s12250-021-00384-w
15. Jackson, C. B., Farzan, M., Chen, B., & Choe, H. (2022). Mechanisms of SARS-CoV-2 entry into cells. *Nature Reviews Molecular Cell Biology, 23*(3), 3-20. https://doi.org/10.1038/s41580-021-00418-x
16. Emeny, J. M., & Morgan, M. J. (1979). Regulation of the interferon system: evidence that Vero cells have a genetic defect in interferon production. *Journal of General Virology, 43*(1), 247-252.
17. Rosli, S. N. Z., Dimeng, S. R., Shamsuddin, F., Mohd Ali, M. R., Muhamad Hendri, N. A., Suppiah, J., Mohd Zain, R., Thayan, R., & Ahmad, N. (2023). Vero CCL-81 and Calu-3 cell lines as alternative hosts for isolation and propagation of SARS-CoV-2 isolated in Malaysia. *Biomedicines, 11*(6), 1658. https://doi.org/10.3390/biomedicines11061658
18. Mautner, L., Hoyos, M., Dangel, A., Berger, C., Ehrhardt, A., & Baiker, A. (2022). Replication kinetics and infectivity of SARS-CoV-2 variants of concern in common cell culture models. *Virology Journal, 19*(1), 76. https://doi.org/10.1186/s12985-022-01802-5
19. Puhach, O., Meyer, B., & Eckerle, I. (2023). SARS-CoV-2 viral load and shedding kinetics. *Nature Reviews Microbiology, 21*(3), 147–161. https://doi.org/10.1038/s41579-022-00822-w
20. Goh, K., Tang, C., Norton, D., & Manivannan, L. (2016). Molecular determinants of plaque size as an indicator of dengue virus attenuation. *Scientific Reports, 6*, 26100. https://doi.org/10.1038/srep26100
21. Pyke, A. T., Nair, N., van den Hurk, A. F., Burtonclay, P., Nguyen, S., Barcelon, J., ... & Prow, N. A. (2021). Replication kinetics of B.1.351 and B.1.1.7 SARS-CoV-2 variants of concern including assessment of a B.1.1.7 mutant carrying a defective ORF7a gene. *Viruses, 13*(6), 1087.
22. Prince, T., Dong, X., Penrice-Randal, R., Randle, N., Hartley, C., Goldswain, H., ... & Hiscox, J. A. (2022). Analysis of SARS-CoV-2 in nasopharyngeal specimens from patients infected with variant B.1.1.7 compared with the wild-type strain in Liverpool, UK. *Journal of Clinical Microbiology, 60*(1), e02592-21. https://doi.org/10.1128/JCM.02592-21
23. Jeong, G. U., Yoon, G. Y., Moon, H. W., Lee, W., Hwang, I., Kim, H., ... Kwon, Y. C. (2022). Comparison of plaque size, thermal stability, and replication rate among SARS-CoV-2 variants of concern. *Viruses, 14*(1), 55. https://doi.org/10.3390/v14010055
24. Guruprasad, K. (2022). Mutations in human SARS-CoV-2 spike proteins, potential drug binding and epitope sites for COVID-19 therapeutics development. *Current Research in Structural Biology, 4*, 41–50. https://doi.org/10.1016/j.crstbi.2022.01.002
25. Liu, Y., Liu, J., Plante, K. S., Plante, J. A., Xie, X., Zhang, X., Ku, Z., An, Z., Scharton, D., Schindewolf, C., Widen, S. G., Menachery, V. D., Shi, P.-Y., & Weaver, S. C. (2022). The N501Y spike substitution enhances SARS-CoV-2 infection and transmission. *Nature, 602*(7896), 294–299. https://doi.org/10.1038/s41586-021-04245-0
26. Lista, M. J., Winstone, H., Wilson, H. D., Dyer, A., Pickering, S., Galao, R. P., De Lorenzo, G., Cowton, V. M., Furnon, W., Suarez, N., Orton, R., Palmarini, M., Patel, A. H., Snell, L., Nebbia, G., Swanson, C., & Neil, S. J. D. (2022). The P681H mutation in the spike glycoprotein of the Alpha variant of SARS-CoV-2 escapes IFITM restriction and is necessary for type I interferon resistance. *Journal of Virology, 96*(23), e0125022. https://doi.org/10.1128/jvi.01250-22
27. Tanneti, N. S., Patel, A. K., Tan, L. H., Marques, A. D., Perera, R. A. P. M., Sherrill-Mix, S., Kelly, B. J., Renner, D. M., Collman, R. G., Rodino, K., Lee, C., Bushman, F. D., Cohen, N. A., & Weiss, S. R. (2024). Comparison of SARS-CoV-2 variants of concern in primary human nasal cultures demonstrates Delta as most cytopathic and Omicron as fastest replicating. *mBio, 15*(4), e0312923. https://doi.org/10.1128/mbio.03129-23
28. Tandel, D., Sah, V., Singh, N. K., Potharaju, P. S., Gupta, D., Shrivastava, S., Sowpati, D. T., & Harshan, K. H. (2022). SARS-CoV-2 variant Delta potently suppresses innate immune response and evades interferon-

activated antiviral responses in human colon epithelial cells. *Microbiology Spectrum, 10*, e01604-22. https://doi.org/10.1128/spectrum.01604-22

29. Shuai, H., Chan, J. F. W., Hu, B., ... & Yuen, K. Y. (2022). Attenuated replication and pathogenicity of SARS-CoV-2 B.1.1.529 Omicron. *Nature, 603*, 693–699. https://doi.org/10.1038/s41586-022-04442-5
30. Zhao, H., Lu, L., Peng, Z., Chen, L. L., Meng, X., Zhang, C., Ip, J. D., Chan, W. M., Chu, A. W., Chan, K. H., Jin, D. Y., Chen, H., Yuen, K. Y., & To, K. K. (2022). SARS-CoV-2 Omicron variant shows less efficient replication and fusion activity when compared with Delta variant in TMPRSS2-expressed cells. *Emerging Microbes & Infections, 11*(1), 277–283. https://doi.org/10.1080/22221751.2021.2023329
31. Bojkova, D., Rothenburger, T., Ciesek, S., Wass, M. N., Michaelis, M., & Cinatl, J. (2022). SARS-CoV-2 Omicron variant virus isolates are highly sensitive to interferon treatment. *Cell Discovery, 8*, 42. https://doi.org/10.1038/s41421-022-00408-z
32. Meng, B., Abdullahi, A., Ferreira, I. A. T. M., ... & Sato, K. (2022). Altered TMPRSS2 usage by SARS-CoV-2 Omicron impacts infectivity and fusogenicity. *Nature, 603*, 706–714. https://doi.org/10.1038/s41586-022-04474-x
33. Motozono, C., Toyoda, M., Zahradnik, J., Saito, A., Nasser, H., Tan, T. S., Ngare, I., Kimura, I., Uriu, K., Kosugi, Y., Yue, Y., Shimizu, R., Ito, J., Torii, S., Yonekawa, A., Shimono, N., Nagasaki, Y., Minami, R., Toya, T., Sekiya, N., ... & Sato, K. (2021). SARS-CoV-2 spike L452R variant evades cellular immunity and increases infectivity. *Cell Host & Microbe, 29*(7), 1124–1136.e11. https://doi.org/10.1016/j.chom.2021.06.006
34. Qu, P., Evans, J. P., Kurhade, C., Zeng, C., Zheng, Y.-M., Xu, K., Shi, P.-Y., Xie, X., & Liu, S.-L. (2023). Determinants and mechanisms of the low fusogenicity and high dependence on endosomal entry of Omicron subvariants. *mBio, 14*(1), e03176-22. https://doi.org/10.1128/mbio.03176-22
35. Sun, C., Wang, H., Yang, J., ... & Luo, M. (2023). Mutation N856K in spike reduces fusogenicity and infectivity of Omicron BA.1. *Signal Transduction and Targeted Therapy, 8*, 75. https://doi.org/10.1038/s41392-022-01281-8
36. Park, S. B., Khan, M., Chiliveri, S. C., ... & Gu, H. (2023). SARS-CoV-2 Omicron variants harbor spike protein mutations responsible for their attenuated fusogenic phenotype. *Communications Biology, 6*, 556. https://doi.org/10.1038/s42003-023-04923-x
37. Koch, J., Uckeley, Z. M., Doldan, P., Stanifer, M., Boulant, S., & Lozach, P. Y. (2021). TMPRSS2 expression dictates the entry route used by SARS-CoV-2 to infect host cells. *The EMBO Journal, 40*(16), e107821. https://doi.org/10.15252/embj.2021107821
38. Aiewsakun, P., Phumiphanjarphak, W., Ludowyke, N., Purwono, P. B., Manopwisedjaroen, S., Srisaowakarn, C., Ekronarongchai, S., Suksatu, A., Yuvaniyama, J., Thitithanyanont, A. (2023). Systematic exploration of SARS-CoV-2 adaptation to Vero E6, Vero E6/TMPRSS2, and Calu-3 cells. *Genome Biology and Evolution, 15*(4), evad035. https://doi.org/10.1093/gbe/evad035
39. Vu, M. N., Lokugamage, K. G., Plante, J. A., Scharton, D., Bailey, A. O., Sotcheff, S., Swetnam, D. M., Johnson, B. A., Schindewolf, C., Alvarado, R. E., Crocquet-Valdes, P. A., Debbink, K., Weaver, S. C., Walker, D. H., Russell, W. K., Routh, A. L., Plante, K. S., & Menachery, V. D. (2022). QTQTN motif upstream of the furin-cleavage site plays a key role in SARS-CoV-2 infection and pathogenesis. *Proceedings of the National Academy of Sciences of the United States of America, 119*(32), e2205690119. https://doi.org/10.1073/pnas.2205690119
40. Romeu, A. R. (2023). Probable human origin of the SARS-CoV-2 polybasic furin cleavage motif. *BMC Genomic Data, 24*(1), 71. https://doi.org/10.1186/s12863-023-01169-8
41. Liu, Z., Zheng, H., Lin, H., Li, M., Yuan, R., Peng, J., Xiong, Q., Sun, J., Li, B., Wu, J., Yi, L., Peng, X., Zhang, H., Zhang, W., Hulswit, R. J. G., Loman, N., Rambaut, A., Ke, C., Bowden, T. A., Pybus, O. G., & Lu, J. (2020). Identification of common deletions in the spike protein of severe acute respiratory syndrome coronavirus 2. *Journal of Virology, 94*(17), e00790-20. https://doi.org/10.1128/JVI.00790-20
42. Davidson, A. D., Williamson, M. K., Lewis, S., ... & Balloux, F. (2020). Characterisation of the transcriptome and proteome of SARS-CoV-2 reveals a cell passage induced in-frame deletion of the furin-like cleavage site from the spike glycoprotein. *Genome Medicine, 12*, 68. https://doi.org/10.1186/s13073-020-00763-0